MSFC-198

Atmospheric Environments for Entry, Descent and Landing (EDL)

C. G. Justus (carl.g.justus@nasa.gov)
Stanley Associates
Natural Environments Branch (EV13)
NASA Marshall Space Flight Center

R.D. Braun (robert.braun@ae.gatech.edu)
School of Aerospace Engineering
Georgia Institute of Technology

June, 2007

1. Introduction

Scientific measurements of atmospheric properties have been made by a wide variety of planetary flyby missions, orbiters, and landers. Although landers can make in-situ observations of near-surface atmospheric conditions (and can collect atmospheric data during their entry phase), the vast majority of data on planetary atmospheres has been collected by remote sensing techniques from flyby and orbiter spacecraft (and to some extent by Earth-based remote sensing). Many of these remote sensing observations (made over a variety of spectral ranges), consist of vertical profiles of atmospheric temperature as a function of atmospheric pressure level. While these measurements are of great interest to atmospheric scientists and modelers of planetary atmospheres, the primary interest for engineers designing entry descent and landing (EDL) systems is information about atmospheric density as a function of geometric altitude. Fortunately, as described more fully in the following section, it is possible to use a combination of the gas-law relation [equation (2.1.1)] and the hydrostatic balance relation [equation (2.1.2)] to convert temperature-versus-pressure, scientific observations into density-versus-altitude data for use in engineering applications.

The following section provides a brief introduction to atmospheric thermodynamics, as well as constituents, and winds for EDL. It also gives methodology for using atmospheric information to do "back-of-the-envelope" calculations of various EDL aeroheating parameters, including peak deceleration rate ("g-load"), peak convective heat rate, and total heat load on EDL spacecraft thermal protection systems. Brief information is also provided about atmospheric variations and perturbations for EDL guidance and control issues, and atmospheric issues for EDL parachute systems.

Subsequent sections give details of the atmospheric environments for five destinations for possible EDL missions: Venus, Earth, Mars, Saturn, and Titan. Specific atmospheric information is provided for these destinations, and example results are presented for the "back-of-the-envelope" calculations mentioned above.

2. Atmospheric Thermodynamics, Constituents, and Winds for EDL

2.1. Atmospheric Temperature

Temperature is the most easily measured (and most familiar) atmospheric parameter. Figure 2.1 shows the wide variety of temperature profiles encountered among the planets and Titan. On the scale of this figure, temperature profiles for Jupiter, Saturn, and Uranus are fairly similar to that for

Neptune, and are not shown. All of our Solar System's planets exhibit a troposphere region, where temperature decreases with altitude, indicative of heat flow upward from the surface (on average). All of our planets exhibit a thermosphere region, where (on average) temperature increases with altitude, because of absorption of heat flux from the Sun as it penetrates into the atmosphere. All of our planets have stratospheres, where temperature decrease above the surface diminishes, and remains relatively constant until the base of the thermosphere (Earth being the exception to this, where the presence of ozone and resultant atmospheric heating produces a local temperature maximum in Earth's stratosphere-mesosphere region).

Although atmospheric temperature has little direct influence on Entry, Descent and Landing (EDL) systems, it is intimately related to the important parameters of atmospheric density and density scale height (discussed in the following two sections). Density (ρ) is related to temperature (T) by the perfect gas law

$$\rho = p\,M / (R_0\,T) \quad , \qquad (2.1.1)$$

where p is atmospheric pressure, M is mean molecular mass, and R_0 is the universal gas constant. In turn, pressure is related to density by the hydrostatic condition

$$dp/dz = -\rho\,g \quad , \qquad (2.1.2)$$

where g is local acceleration of gravity, and z is geometric altitude. From a combination of these two relations, the pressure scale height (H_p) can be derived as

$$H_p = -p / (dp/dz) = R_0\,T / (M\,g) \quad . \qquad (2.1.3)$$

In the simplified case of an isothermal (constant temperature) atmosphere, density as a function of altitude is given by

$$\rho(z) = \rho(0)\ \exp(-\,z / H_p) \qquad \text{[isothermal]} \quad . \qquad (2.1.4)$$

Atmospheric temperature also determines sound speed, c, by the relation

$$c = [\,(C_p/C_v)\,R_0\,T / M\,]^{1/2} \quad , \qquad (2.1.5)$$

where C_p and C_v are specific heats at constant pressure and volume, respectively. From equation (2.1.1), c may also be expressed as

$$c = [\,(C_p/C_v)\,p / \rho\,]^{1/2} \quad . \qquad (2.1.6)$$

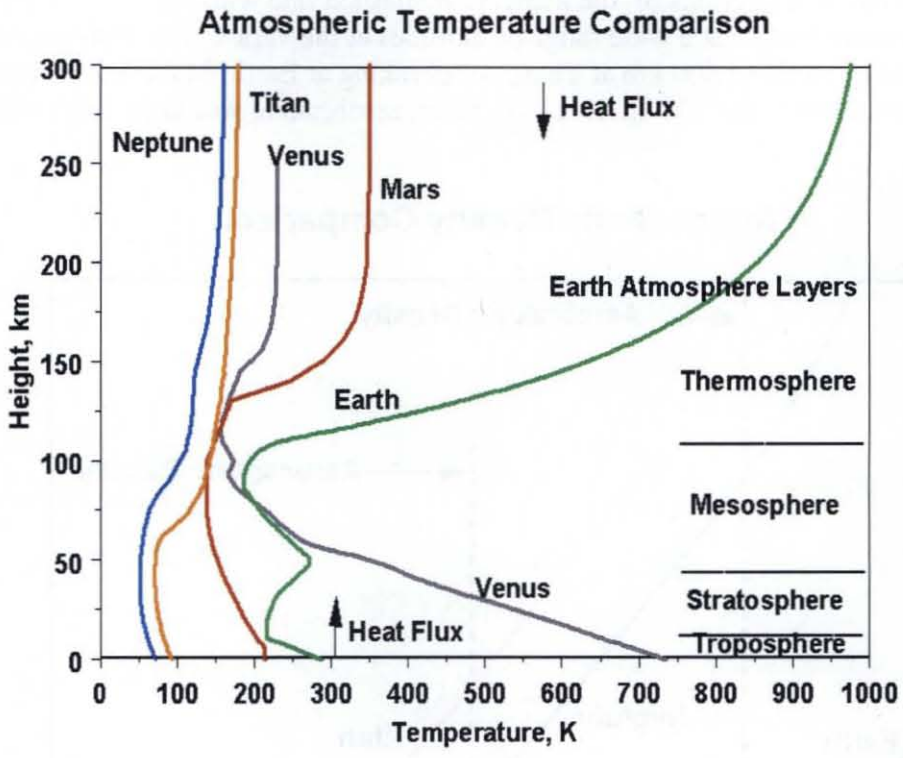

Figure 2.1 - Comparison of temperature profiles among the planets and Titan.

2.2. Atmospheric Density

All EDL technologies are affected by atmospheric drag. Atmospheric drag force (D) is proportional to atmospheric density

$$D = - C_D \rho V^2 A / 2 \quad , \qquad (2.2.1)$$

where C_D is the drag coefficient, V is spacecraft velocity with respect to the atmosphere, and A is effective cross-sectional area of the spacecraft. For lifting bodies, lift force (L) is also proportional to atmospheric density

$$L = - C_L \rho V^2 A / 2 \quad , \qquad (2.2.2)$$

where C_L is the lift coefficient. Relative importance of lift is characterized by the lift-to-drag ratio (L/D)

$$L/D = C_L / C_D \quad . \qquad (2.2.3)$$

Figure 2.2 compares atmospheric density profiles among the planets and Titan. Vertical dashed lines in this figure indicate typical density values at which aerocapture or aerobraking operations would occur. Aerocapture is the process of using one drag-pass through the atmosphere to slow down from interplanetary transfer orbit to a captured orbit. Aerobraking is the process of using many (lower density) drag-passes through the atmosphere to gradually circularize a highly elliptical

(but captured) orbit. Intersections of the aerocapture dashed line with various density curves shows that aerocapture would occur at a wide range of altitudes at the various destinations, varying from about 50 km at Mars to about 300 km at Titan. Aerobraking at Earth, Mars, and Venus would take place near, and just above, the 100 km level. At Titan, aerobraking would be implemented near 700 km.

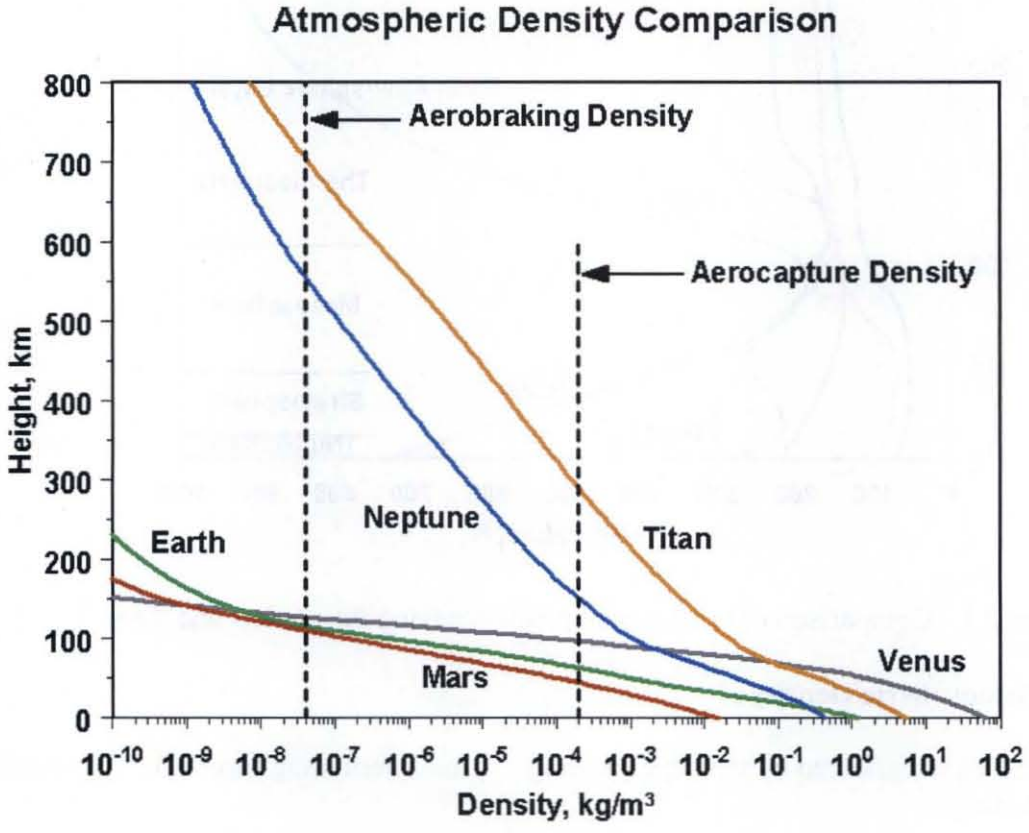

Figure 2.2 - Comparison of atmospheric density profiles among the planets and Titan.

2.3. Density Scale Height

Density scale height (H_ρ) is defined, analogous to pressure scale height in equation (2.1.3), by

$$H_\rho = - \rho / (d\rho/dz) \quad . \qquad (2.3.1)$$

For the general case when temperature (and possibly molecular mass) varies with altitude, density scale height is related to pressure scale height by

$$H_\rho = H_p / [\, 1 + (H_p / T)\, dT/dz - (H_p / M)\, dM/dz \,] \quad . \qquad (2.3.2)$$

For isothermal atmospheres with constant molecular mass, H_p and H_ρ would be identical. For the simplified case of constant density scale height, density versus altitude is given by

$$\rho(z) = \rho(0)\ \exp(- z / H_\rho) \qquad [\text{constant } H_\rho] \quad . \qquad (2.3.3)$$

Figure 2.2 shows that density decreases fairly rapidly with altitude for the terrestrial planets (Venus, Earth, Mars), while it decreases rather slowly for Titan. This effect is explained by differences in density scale height, for the various planets and Titan. From equation (2.3.3), density decreases rapidly with altitude if H_ρ is small, while it decreases slowly if H_ρ is large. From equations (2.3.2) and (2.1.3), H_ρ is proportional to pressure scale height [$R_0 T / (M g)$]. For the terrestrial planets, molecular mass M is large ($M \approx 29$-44), so H_ρ is small. For Titan, H_ρ is large, despite its low temperature and high molecular mass ($M \approx 29$), because its gravity (g) is low.

Next to density itself, density scale height is the most important atmospheric parameter affecting EDL systems. For example, density scale height is important in determining corridor width, or entry angle range that allows the vehicle to achieve desired surface landing zone, without "skipping out" or "burning in". Rapid density variation with altitude (small density scale height) allows little "room to maneuver", while slow density variation with altitude (large density scale height) makes for a large corridor width. As discussed in Section 2.6, density scale height also plays a direct role in determining many other factors relevant to EDL, such as:

- height where maximum deceleration (g-load) occurs
- height where maximum convective heat flux occurs
- magnitude of maximum g-load
- magnitude of maximum convective heat flux
- magnitude of total convective heat load
- sensitivity of max g-load, max heat flux, and total heat load to changes in entry flight path angle

If density values ρ_1 and ρ_2 are known at heights z_1 and z_2, then density scale height, applicable over the height range from z_1 to z_2, can be calculated using the relation

$$H_\rho = (z_2 - z_1) / ln(\rho_1 / \rho_2) \quad . \qquad (2.3.4)$$

2.4. Atmospheric Composition

Atmospheric composition determines mean molecular mass M, which in turn affects density [equation (2.1.1)], pressure scale height [equation (2.1.3)], and density scale height [equation (2.3.2)]. For an atmosphere consisting of n major species, with molecular masses M_i (i = 1 to n), with mole fractions (or volume fractions) f_i, mean molecular mass is given by

$$M = \sum_{i=1}^{n} f_i \, M_i \quad , \qquad (2.4.1)$$

where

$$\sum_{i=1}^{n} f_i = 1 \quad . \qquad (2.4.2)$$

Atmospheric composition also plays an important role in determining the convective heat flux coefficient (Sutton and Graves, 1971). Even minor species can play an important role in radiative heating, since some minor species can be very active radiatively. Some species that strongly affect

radiative heat flux (e.g. the CN radical in Titan's atmosphere) are not present naturally, but are produced by thermochemical reactions due to interaction of the spacecraft with the atmosphere.

2.5. Winds

Many EDL operations occur at very high speeds. In this case, it is only if wind speed (W) becomes non-negligible with respect to spacecraft velocity (V) that wind plays an important role. Since W can never exceed a substantial fraction of the speed of sound, wind becomes important only when V becomes subsonic, or at most when V is near the speed of sound. An important application for which wind is important is deployment and operation of parachutes during final (low speed) stages of entry and landing.

2.6. EDL Aeroheating Environments

For the short course on planetary entry, descent, and landing (EDL), Braun (2004) used methodology developed by Allen and Eggers (1959) to derive "back of the envelope" solutions to the equations of motion, applicable for EDL. For low L/D EDL, spacecraft velocity, V, as a function of altitude, z, is given by

$$V(z) = V_{atm} \exp[\, C \exp(-z / H_s)\,] \quad , \qquad (2.6.1)$$

where $H_s = H_\rho$ of equation (2.3.3) is (constant) density scale height, V_{atm} is spacecraft velocity at atmospheric interface, coefficient C is given by

$$C = \rho(0)\, H_s / [\, 2\, \beta \sin(\gamma)\,] \quad , \qquad (2.6.2)$$

$\rho(0)$ is density at height 0, given by equation (2.3.3), β is ballistic coefficient, given by

$$\beta = m / (C_D\, A) \quad , \qquad (2.6.3)$$

where m is spacecraft mass, A is effective cross-sectional area, and C_D is drag coefficient, defined by equation (2.2.1). Flight path angle γ in equation (2.6.2) is the angle from the horizontal plane to the direction of the flight path. Angle γ is negative for EDL flight paths. With negative γ, coefficient C in equation (2.6.2) is also negative. Note that $\rho(0)$ in equation (2.6.2) is not necessarily the same as surface atmospheric density, it can be just a parameter for use in equation (2.3.3), with density scale height computed from equation (2.3.4), in which case density from this relation would be valid only within the altitude range from z1 to z2 of equation (2.3.4).

Atmospheric interface velocity in equation (2.6.1) is given by

$$V_{atm} = [\, V_\infty^2 + 2\, \mu / r_{atm}\,]^{1/2} \quad , \qquad (2.6.4)$$

where V_∞ is the spacecraft velocity "at infinity" (i.e. far from the planet's sphere of influence). V_∞ is related to the orbital kinetic energy per unit mass (usually denoted C_3), since

$$C_3 = V_\infty^2 / 2 \quad . \qquad (2.6.5)$$

In equation (2.6.4), μ is the planetary gravitational parameter, and r_{atm} is the radius from the center of the planet to atmospheric interface altitude. μ is given by

$$\mu = G M_p \quad , \qquad (2.6.6)$$

where G is Newton's gravitational constant and M_p is the planetary mass. Escape velocity (for escape from atmospheric interface altitude) is given by

$$V_{esc} = [2 \mu / r_{atm}]^{1/2} \quad , \qquad (2.6.7)$$

so equation (2.6.4) can also be written

$$V_{atm} = [V_\infty^2 + V_{esc}^2]^{1/2} \quad . \qquad (2.6.8)$$

From this result, we see that V_{atm} always equals or exceeds escape velocity. Equations (2.6.4) and (2.6.8) assume that EDL is accomplished by direct entry from an interplanetary transfer orbit. If entry occurs from a captured orbit (as in the case of Viking entries at Mars), then V_{atm} is determined by characteristics of the captured orbit, and V_{atm} will be less than V_{esc}.

As shown by Braun (2004), the approximate velocity solution provided by equation (2.6.1) can be used to estimate a number of parameters of interest to EDL. The maximum g-load (acceleration in Earth g's) is given by

$$gmax = [V_{atm}^2 \sin(\gamma)] / [53.31 H_s] \quad . \qquad (2.6.9)$$

Since γ is negative, this represents a deceleration on the spacecraft. Altitude z(gmax), at which maximum g-load occurs, is given by

$$z(gmax) = H_s \ln(- 2 C) \quad . \qquad (2.6.10)$$

Velocity at which gmax occurs is

$$V(gmax) = 0.6065 V_{atm} \quad . \qquad (2.6.11)$$

Substitution of equation (2.6.10) into equation (2.3.3) shows that the atmospheric density where gmax occurs is

$$\rho(gmax) = \rho(0) \exp[- \ln (- 2 C)] = \beta \sin(\gamma) / H_s \quad . \qquad (2.6.12)$$

Convective heat flux to the stagnation point on the nose of the spacecraft is given by

$$q = k (\rho / r_n)^{1/2} V^3 \quad , \qquad (2.6.13)$$

where k is the convective heat transfer coefficient (which depends on atmospheric constituents), and r_n is the spacecraft nose radius.

Approximate velocity solution equation (2.6.1) can also be used to show that the height at which maximum convective heat flux (qmax) occurs is

$$z(qmax) = H_s \ln(- 6 C) \quad , \qquad (2.6.14)$$

while the velocity and density at qmax are given by

$$V(qmax) = 0.8465 V_{atm} \quad , \qquad (2.6.15)$$

and

$$\rho(qmax) = \rho(0) \exp[- \ln (- 6 C)] = \beta \sin(\gamma) / (3 H_s) \quad . \qquad (2.6.16)$$

These results show that qmax occurs at higher altitude (higher velocity and lower density) than does maximum g-load. Substitution of equations (2.6.15) and (2.6.16) into equation (2.6.13) yields maximum stagnation convective heat flux, given by

$$qmax = k [\rho(qmax) / r_n]^{1/2} V(qmax)^3$$

$$= 0.3502 k [- \beta \sin(\gamma) / (H_s r_n)]^{1/2} V_{atm}^3 \quad . \qquad (2.6.17)$$

Total convective heat load, Q, can also be found from velocity solution (2.6.1), by integration of equation (2.6.13)

$$Q = \int_{-\infty}^{\infty} q(t) \, dt = \int_{0}^{\infty} \{ q(z) / [V(z) \sin(\gamma)] \} \, dz \quad , \qquad (2.6.18)$$

which yields the result

$$Q = k \{ - \pi \beta H_s / [r_n \sin(\gamma)] \}^{1/2} V_{atm}^3 \quad . \qquad (2.6.19)$$

Velocity solution (2.6.1) and all the parameters derived from that equation are based on the assumption that flight path angle γ is constant. Allen and Eggers (1959) showed that this assumption is valid for EDL trajectories over the height range encompassing gmax and qmax.

The solutions above also assume low lift (low L/D) entry bodies. Although Braun (2004) provides some results for lifting bodies, details of the effects of L/D are beyond the scope of this report. Some general conclusions about effects of L/D are that it:

- significantly reduces maximum g-load (gmax)
- lowers the maximum convective heat flux at the stagnation point (qmax)
- raises the altitudes at which gmax and qmax occur
- increases the total heat load (Q)

In addition to convective heat flux and heat load, Braun (2004) also briefly discusses radiative heat flux and heat load. However, these parameters involve many complicated processes, and are also beyond the scope of this report.

2.7 Atmospheric Variations and Perturbations: EDL Guidance and Control Issues

Atmospheres undergo variability and perturbations on a wide range of spatial and temporal scales. In terms of spatial scales, variations range from global in dimension (e.g. changes between polar and equatorial latitudes) , to intermediate-scale, wave-like variations of various types, to small-scale turbulence (down to a few meters or smaller in dimension). Time scales range from long-period seasonal changes, to intermediate-period (approximately diurnal) variations, to small-scale waves and turbulence having time scales of a few minutes or shorter.

Large-scale variations can affect thermal protection systems for EDL. For example, if an entry spacecraft first encounters lower-than-normal density, it will accelerate to higher-than-normal speed. If, because of large-scale atmospheric variations, it subsequently encounters higher-than-normal density at the new higher-than normal speed, this can cause significant increase in convective heat flux [via equation (2.6.13)].

Intermediate-to-small-scale atmospheric perturbations can affect both unguided and guided entry systems. Some effects include:

- Spacecraft attitude stability (for both unguided and guided entry)
- Landing footprint dispersion size (for both unguided and guided entry)
- Design parameters for entry guidance and control systems and algorithms for guided entry

Complete details of atmospheric variations and perturbations, how they vary from planet to planet, and their effects on entry systems, are beyond the scope of this paper.

2.8 Atmospheric Issues for EDL Parachute Systems

Virtually all EDL spacecraft rely on parachutes for at least part of their deceleration prior to landing. At high (supersonic) initial speeds, parachute deploy may be triggered when a specific Mach number (spacecraft speed relative to speed of sound) is reached. For these purposes, speed of sound, can be evaluated by equations (2.1.5) or (2.1.6), with representative values provided in tables given in the following sections. Parachute deploy can also be triggered by an on-board accelerometer (or "g-switch"), where spacecraft deceleration is determined by the amount of atmospheric drag, given by equation (2.2.1). A potential issue is the possibility for "spoofing" of the parachute deploy system by small-to-intermediate scale atmospheric perturbations. For example, sufficient density (and drag) may be encountered to trigger parachute deploy, but if atmospheric perturbations are of sufficiently large amplitude, a subsequent density may be encountered that is too low for proper parachute operation. These aspects can be addressed by Monte-Carlo simulations of realistic atmospheric perturbations, with assessment of engineering factors such as "dead band" in the parachute deploy trigger system (e.g. allowing sufficient delay after encountering critical drag density to ensure that "spoofing" problems will not occur). During early entry phase (high altitude) segments of the trajectory, density is the most critical atmospheric parameter. During later entry phase (low altitude), and particularly after parachute deploy, horizontal winds (and to a lesser extent, vertical winds) are the most critical atmospheric parameter.

A critical entry operation after parachute deploy is the amount of spacecraft drift due to horizontal winds. Large-to-intermediate-scale wind variations cause horizontal drift that affects the overall size of the landing ellipse (both along-track and across-track). In addition, intermediate-to-small-

scale atmospheric perturbations can affect landing system stability (e.g. by inducing undesirable oscillations in the spacecraft while it is on parachute).

3. Venus Environment

3.1. Venus Neutral Atmosphere

The following material gives a summary of Venus atmospheric information, including results of some calculations using "back of the envelope" methods presented in Section 2.6. For more complete information on atmospheric properties, and how they vary with height, latitude, season, etc., the Venus Global Reference Atmospheric Model (Venus-GRAM) is available (Justus et al., 2004a; Duvall et al., 2005).

3.1.1. Venus Atmospheric Temperature

From data observed by Magellan, other Venus orbiters, and several entry probes, Kliore et al. (1986) have developed a "Venus International Reference Atmosphere" (VIRA). Table 3.1.1 shows an abbreviated table of density, temperature, and sound speed versus altitude from the VIRA model. In the calculation of sound speed, from equation (2.1.5) or equation (2.1.6), the ratio of specific heats C_p/C_v is 1.286 for Venus.

Table 3.1.1 - Mean density, temperature, and sound speed from VIRA model

Height (km)	Density (kg/m3)	Temperature (K)	Sound Speed (m/s)
0	6.48E+01	735.3	427.6
10	3.77E+01	658.2	402.0
20	2.04E+01	580.7	376.9
30	1.02E+01	496.9	348.4
40	4.40E+00	417.6	319.7
50	1.59E+00	350.5	293.3
60	4.69E-01	262.8	254.1
70	8.39E-02	229.8	237.8
80	1.19E-02	197.1	220.3
90	1.15E-03	169.4	204.3
100	7.99E-05	173.9	207.2
110	5.81E-06	158.0	197.1
120	3.20E-07	159.0	199.2
130	1.85E-08	166.8	209.1
140	1.39E-09	176.2	233.9
150	1.61E-10	194.2	276.0

3.1.2. Venus Atmospheric Density

Table 3.1.1 gives Venus atmospheric density as a function of height, from the VIRA model (Kliore et al., 1986). At low altitudes (0-100 km), VIRA density and temperature depend on latitude only. For middle altitudes (100-150 km), dependence is on time-of-day only. For high altitudes (150-250 km), VIRA density and temperature depend on solar zenith angle only.

Over the height range 75-150 km, best fit density versus height, assuming constant scale height according to equation (2.3.3), yields $\rho(0) = 1.369E+7$ kg/m^3 and $H_\rho = 3.831$ km. Note that parameter $\rho(0)$ for this density fit differs markedly from true surface density given in Table 3.1.1. This is due to the fact that, as shown in the next section, the assumption of constant scale height is not valid below 75 km.

3.1.3. Venus Density Scale Height

Table 3.1.2 gives Venus density scale height as a function of altitude, from the VIRA model (Kliore et al., 1986). This table shows that the assumption of constant scale height breaks down below 75 km, illustrating why the density fit given in the previous section (valid only between 75 and 150 km) gives a value of $\rho(0)$ that differs markedly from the true surface density value (given in Table 3.1.1).

Table 3.1.2 - Density scale height from VIRA model

Height (km)	Density Scale Height (km)
0	19.10
10	17.27
20	15.35
30	13.20
40	10.74
50	9.32
60	6.26
70	5.44
80	4.66
90	4.00
100	3.63
110	3.60
120	3.44
130	3.63
140	4.29
150	4.70

3.1.4. Venus Atmospheric Composition

From the "Venus Fact Sheet" (National Space Science Data Center, 2004), atmospheric composition (mole fraction or volume fraction) near the surface is: 96.5% carbon dioxide (CO_2), 3.5% nitrogen (N_2), with minor constituents sulfur dioxide (SO_2) - 150 ppm ; argon (Ar) - 70 ppm; water vapor (H_2O) - 20 ppm; carbon monoxide (CO) - 17 ppm; helium (He) - 12 ppm; and neon (Ne) - 7 ppm. Near-surface mean molecular mass is 43.45 g/mole (43.45 kg/k-mole).

Above about 100 km altitude, the constituent mix begins to vary with altitude, as given in Figure 3.1.1. Eventually, because of the effects of diffusive separation at very high altitudes, the atmosphere of Venus becomes primarily atomic hydrogen (H) and helium (He).

Between approximately 45 and 70 km altitude, a dense cloud layer covers the planet Venus. Sulfuric acid cloud droplets, composed of about 75% hydrogen sulfide and 25% water, have sizes

ranging from about 1 μm to 10 μm. Because these sulfuric acid droplets are confined to below about 70 km, they have no effect on aerobraking or aerocapture at Venus, but may be an important consideration for EDL.

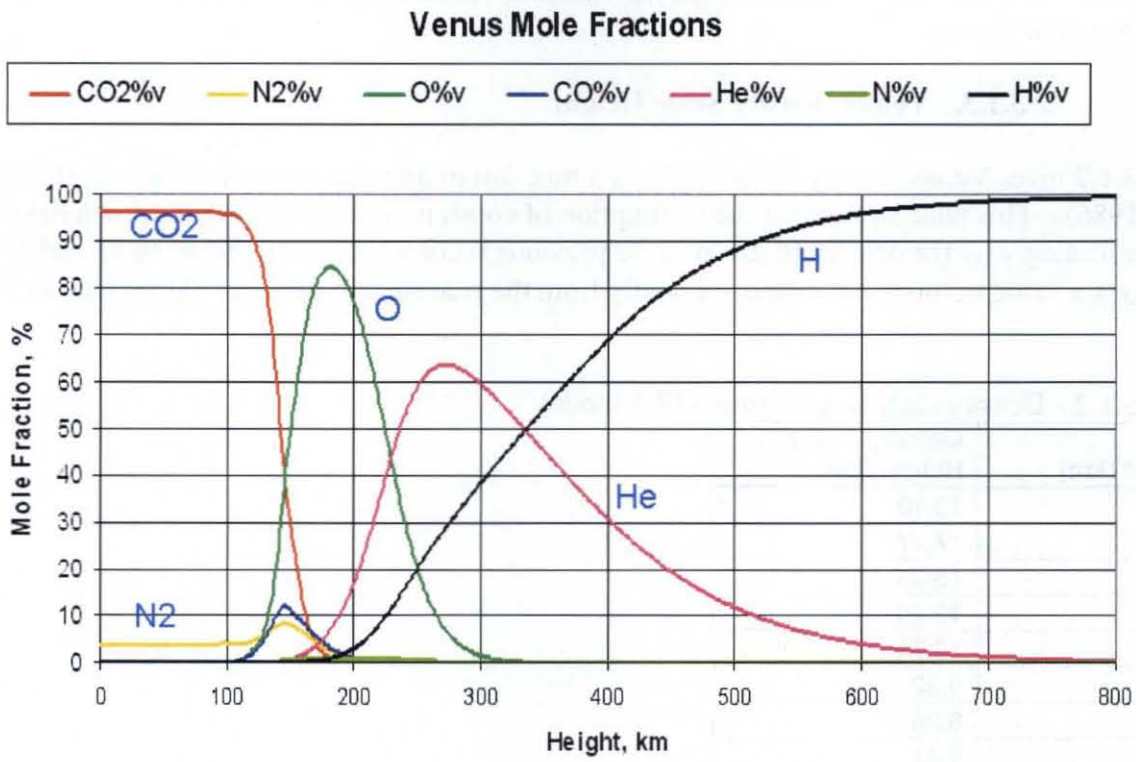

Figure 3.1.1 - Altitude variation of Venus atmospheric constituents.

3.1.5. Venus Winds

Below about 100 km altitude, winds on Venus are dominated by a "superrotating" component. Since Venus rotation is retrograde (East-to-West), winds in this height region are also retrograde. At higher altitudes, Venus winds are dominated by flow that upwells from near the sub-solar point and travels in all directions around the planet, finally subsiding near the anti-solar point. The vertical profile of mean wind on Venus is illustrated in Figure 3.1.2. Near 100 km altitude, total winds are approximately 100 m/s or less. These winds may be compared to sound speed at this altitude of ~200 m/s, as given in Table 3.1.1.

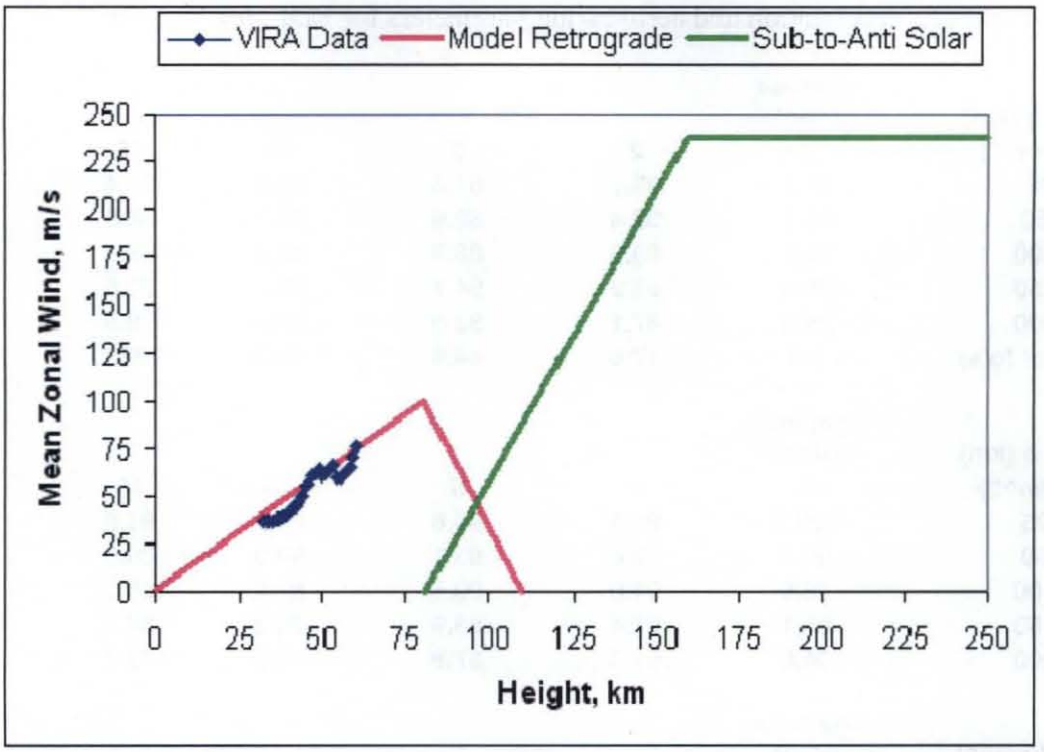

Figure 3.1.2 - Vertical profile of mean wind on Venus (winds up to about 100 km are retrograde, East to West).

3.2. Venus Aeroheating Environments

Sections 2.6.1 through 2.6.3 present methodologies for doing "back of the envelope" calculations of various parameters related to deceleration and aeroheating environments for EDL (Braun, 2004). Parameters relevant to EDL, computed by the methodology of Section 2.6.1, are given in Table 3.2.1 (for $V_\infty = 0$) and Table 3.2.2 (for $V_\infty = 5$ km/s). For these tables, density (for heights 75 km to 150 km) was computed by parameters given in Section 3.1.2. Atmospheric interface altitude was taken as 135 km. For heat flux and heat load, a spacecraft nose radius value of 1 m was used. Results in these tables should be used for comparative purposes only, not for spacecraft design.

These tables give several parameters versus beta [ballistic coefficient β, defined by equation (2.6.3)] and gamma [γ, the flight path angle]. Parameters given are "Hgt Max g" [altitude of maximum g-load, z(gmax) from equation (2.6.10)], "Max Decel" {magnitude of maximum deceleration, gmax from equation (2.6.9)], "Hgt Max q" [altitude of maximum convective heat flux to stagnation point, z(qmax) from equation (2.6.14)], "qmax" [maximum convective heat flux at stagnation point, qmax from equation (2.6.17)], and "Qtot" [total heat load on stagnation point, Q from equation (2.6.19)].

Table 3.2.1 - Venus deceleration and aeroheating parameters for EDL, for $V_\infty = 0$

Hgt Max g (km)	-gamma (deg)				
beta (kg/m^2)	1	2	5	10	15
25	97.7	95.1	91.6	88.9	87.4
50	95.1	92.4	88.9	86.3	84.8
100	92.4	89.8	86.3	83.6	82.1
150	90.9	88.2	84.7	82.1	80.6
200	89.8	87.1	83.6	81.0	79.5
Max Decel (g's)	9.0	17.9	44.8	89.3	133.1

Hgt max q (km)	-gamma (deg)				
beta (kg/m^2)	1	2	5	10	15
25	102.0	99.3	95.8	93.2	91.6
50	99.3	96.6	93.1	90.5	89.0
100	96.6	94.0	90.5	87.8	86.3
150	95.1	92.4	88.9	86.3	84.8
200	94.0	91.3	87.8	85.2	83.7

qmax (W/cm^2)	-gamma (deg)				
beta (kg/m^2)	1	2	5	10	15
25	44.2	62.5	98.7	139.4	170.2
50	62.5	88.4	139.6	197.1	240.6
100	88.4	125.0	197.5	278.8	340.3
150	108.2	153.1	241.9	341.4	416.8
200	125.0	176.7	279.3	394.2	481.3

Qtot (kJ/cm^2)	-gamma (deg)				
beta (kg/m^2)	1	2	5	10	15
25	8.30	5.87	3.71	2.63	2.15
50	11.73	8.30	5.25	3.72	3.05
100	16.60	11.74	7.43	5.26	4.31
150	20.33	14.37	9.10	6.44	5.28
200	23.47	16.60	10.50	7.44	6.09

Table 3.2.2 - Venus deceleration and aeroheating parameters for EDL, for V_∞ = 5 km/s

Hgt Max g (km)	-gamma (deg)				
beta (kg/m^2)	1	2	5	10	15
25	97.7	95.1	91.6	88.9	87.4
50	95.1	92.4	88.9	86.3	84.8
100	92.4	89.8	86.3	83.6	82.1
150	90.9	88.2	84.7	82.1	80.6
200	89.8	87.1	83.6	81.0	79.5
Max Decel (g's)	11.1	22.2	55.5	110.6	164.8

Hgt max q (km)	-gamma (deg)				
beta (kg/m^2)	1	2	5	10	15
25	102.0	99.3	95.8	93.2	91.6
50	99.3	96.6	93.1	90.5	89.0
100	96.6	94.0	90.5	87.8	86.3
150	95.1	92.4	88.9	86.3	84.8
200	94.0	91.3	87.8	85.2	83.7

qmax (W/cm^2)	-gamma (deg)				
beta (kg/m^2)	1	2	5	10	15
25	60.9	86.1	136.0	192.0	234.4
50	86.1	121.7	192.4	271.5	331.5
100	121.7	172.1	272.0	384.0	468.8
150	149.1	210.8	333.2	470.3	574.2
200	172.2	243.5	384.7	543.1	663.0

Qtot (kJ/cm^2)	-gamma (deg)				
beta (kg/m^2)	1	2	5	10	15
25	10.27	7.26	4.60	3.26	2.67
50	14.53	10.27	6.50	4.61	3.77
100	20.55	14.53	9.19	6.51	5.34
150	25.16	17.79	11.26	7.98	6.53
200	29.06	20.55	13.00	9.21	7.55

4. Earth Environment

4.1. Earth Neutral Atmosphere

The following material gives a summary of Earth atmospheric information, including results of some calculations using "back of the envelope" methods presented in Section 2.6. For more complete information on atmospheric properties, and how they vary with height, latitude, season, etc., the Earth Global Reference Atmospheric Model (Earth-GRAM) is available (Justus et al., 2004b; Duvall et al., 2005).

4.1.1. Earth Atmospheric Temperature

Table 4.1.1 shows an abbreviated table of density, temperature, density scale height, and sound speed versus altitude from the U.S. Standard Atmosphere (National Oceanic and Atmospheric Administration, National Aeronautics and Space Administration, and United States Air Force, 1976) . In the calculation of sound speed, from equation (2.1.5) or equation (2.1.6), the ratio of specific heats C_p/C_v is 1.40 for Earth.

Table 4.1.1 - Mean density, temperature, density scale height, and sound speed from 1976 US Standard Atmosphere

Height (km)	Density (kg/m^3)	Temperature (K)	Density Scale Height (km)	Sound Speed (m/s)
0	1.225E+00	288.1	10.20	340.3
10	4.135E-01	223.3	7.66	299.5
20	8.891E-02	216.6	6.31	295.1
30	1.841E-02	226.5	6.50	301.7
40	3.996E-03	250.3	6.86	317.2
50	1.027E-03	270.6	8.14	329.8
60	3.097E-04	247.0	8.02	315.1
70	8.283E-05	219.6	7.14	297.1
80	1.846E-05	198.6	6.33	282.5
90	3.416E-06	186.9	5.62	274.1
100	5.604E-07	195.1	5.57	280.0
110	9.708E-08	240.0	5.69	310.6
120	2.222E-08	360.0	8.38	380.4
130	8.152E-09	469.3	11.71	434.3
140	3.831E-09	559.6	14.86	474.2
150	2.076E-09	634.4	17.70	504.9

4.1.2. Earth Atmospheric Density

Over the height range 0 km to 100 km, best fit density versus height, assuming constant scale height according to equation (2.3.3), yields $\rho(0) = 1.226\ kg/m^3$ and $H_\rho = 7.256$ km. Note that parameter $\rho(0)$ for this density fit agrees closely with the true surface density given in Table 4.1.1. This is due to the fact that, up to about 100 km, density scale height is fairly constant. Although density values provided by this fit are adequate for EDL, a different density fit for heights near and above 100 km would be more suitable for aerobraking applications.

Due to variations in location and season, density profiles may differ significantly (up to a few 10s of percent) from the US Standard Atmosphere values in Table 4.1.1. For more complete information on this variability, the Earth Global Reference Atmospheric Model (Earth-GRAM) is recommended (Justus et al., 2004b; Duvall et al., 2005).

4.1.3. Earth Density Scale Height

Table 4.1.1 gives Earth atmospheric density scale height as a function of altitude. This table shows that the assumption of constant scale height breaks down above about 100 km, illustrating why the

density fit given in the previous section (valid only between 0 km and 100 km) would not be suitable for use above about 100 km.

4.1.4. Earth Atmospheric Composition

From the "Earth Fact Sheet" (National Space Science Data Center, 2004), atmospheric composition (mole fraction or volume fraction) near the surface is: 78.084% nitrogen (N_2), 20.946% oxygen (O_2), with minor constituents: argon (Ar) - 9340 ppm; carbon dioxide (CO_2) - 350 ppm; neon (Ne) - 18.18 ppm; helium (He) - 5.24 ppm; CH_4 - 1.7 ppm; krypton (Kr) - 1.14 ppm; and hydrogen (H_2) - 0.55 ppm. Water vapor, which is highly variable, typically makes up about 1%. Near-surface mean molecular mass is 28.97 g/mole (28.97 kg/k-mole).

Above about 100 km altitude, the constituent mix begins to vary with altitude, as given in Figure 4.1.1. Eventually, because of the effects of diffusive separation at very high altitudes, the atmosphere of Earth becomes primarily atomic hydrogen (H), helium (He), and atomic oxygen (O). At orbital altitudes between about 300 km and 500 km, atomic oxygen is present in large enough concentrations to cause concern for some satellite materials. However, for altitudes of concern for EDL, atomic oxygen is not a factor.

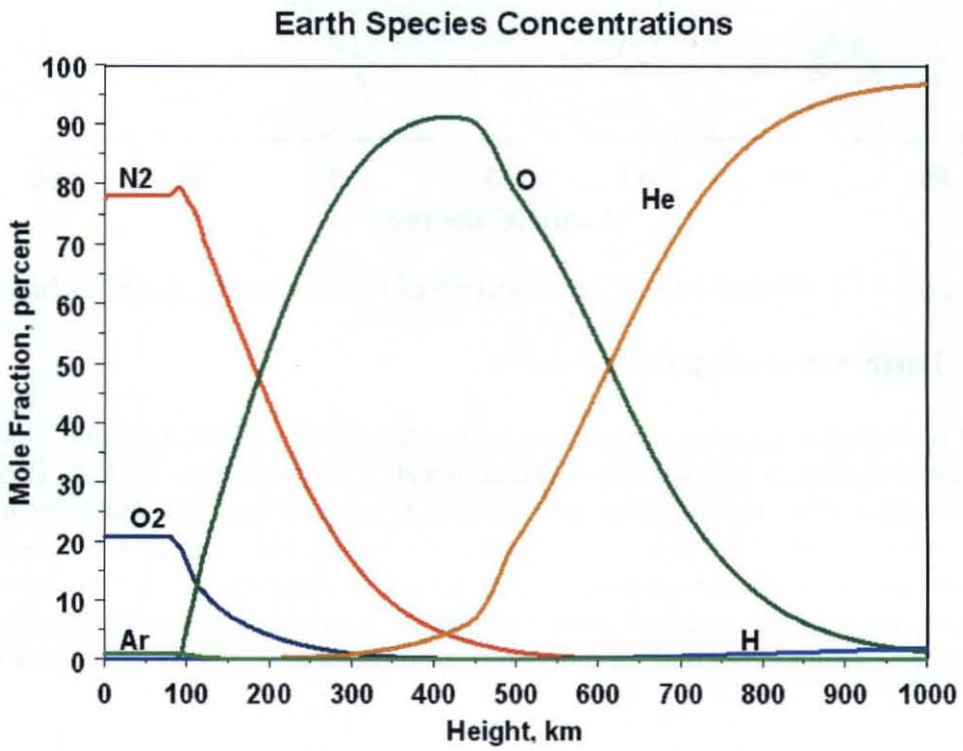

Figure 4.1.1 - Altitude variation of Earth atmospheric constituents.

4.1.5. Earth Winds

Figure 4.1.2 shows a height-latitude cross section of Earth eastward winds for July (northern hemisphere summer, southern hemisphere winter). This figure shows that Earth winds vary considerably with height, latitude and season. However, comparison with values of sound speed,

from Table 4.1.1, shows that winds are a factor only when spacecraft speeds are well below sonic magnitude.

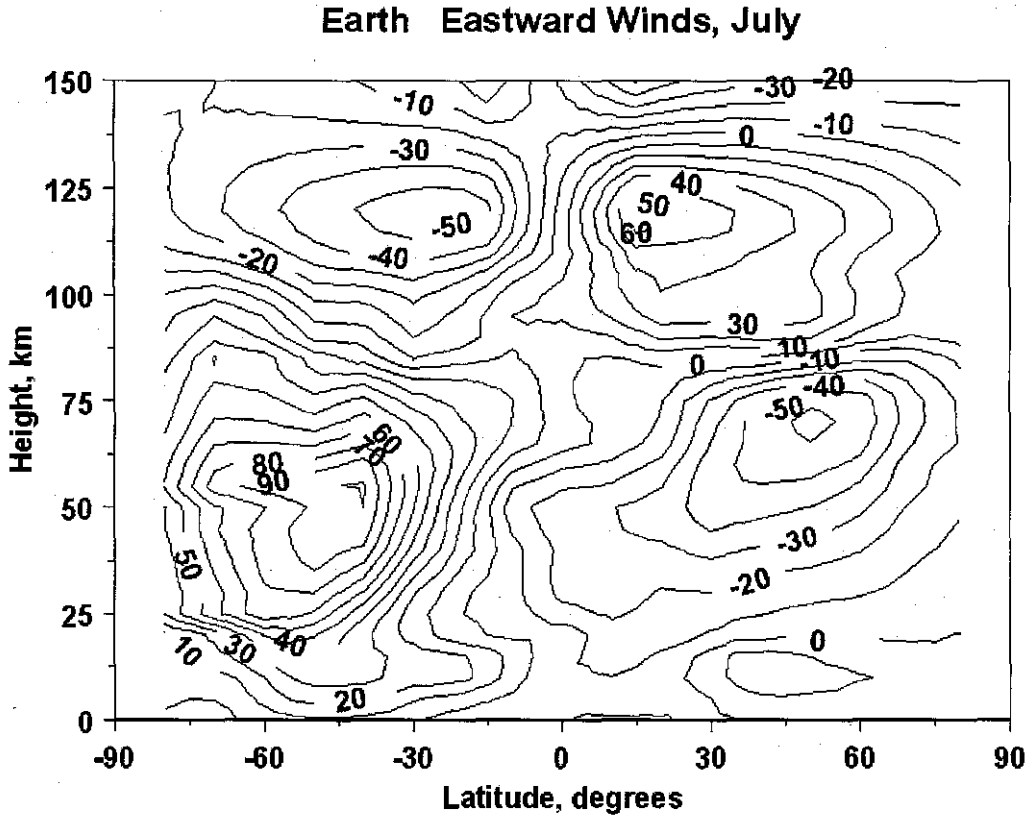

Figure 4.1.2 - Height-latitude cross section of Earth eastward winds for July.

4.2. Earth Aeroheating Environments

Sections 2.6.1 through 2.6.3 present methodologies for doing "back of the envelope" calculations of various parameters related to deceleration and aeroheating environments for EDL (Braun, 2004). Parameters relevant to EDL, computed by the methodology of Section 2.6.1, are given in Table 4.2.1 (for $V_\infty = 0$) and Table 4.2.2 (for $V_\infty = 5$ km/s). For these tables, density (for heights 0 km to 100 km) was computed by parameters given in Section 4.1.2. Atmospheric interface altitude was taken as 140 km. For heat flux and heat load, a spacecraft nose radius value of 1 m was used. Results in these tables should be used for comparative purposes only, not for spacecraft systems design.

These tables give several parameters versus beta [ballistic coefficient β, defined by equation (2.6.3)] and gamma [γ, the flight path angle]. Parameters given are "Hgt Max g" [altitude of maximum g-load, z(gmax) from equation (2.6.10)], "Max Decel" [magnitude of maximum deceleration, gmax from equation (2.6.9)], "Hgt Max q" [altitude of maximum convective heat flux to stagnation point, z(qmax) from equation (2.6.14)], "qmax" [maximum convective heat flux at stagnation point, qmax from equation (2.6.17)], and "Qtot" [total heat load on stagnation point, Q from equation (2.6.19)].

Table 4.2.1 - Earth deceleration and aeroheating parameters for EDL, for $V_\infty = 0$

Hgt Max g (km)	-gamma (deg)				
beta (kg/m^2)	1	2	5	10	15
25	72.0	67.0	60.3	55.3	52.4
50	67.0	62.0	55.3	50.3	47.4
100	61.9	56.9	50.3	45.3	42.4
150	59.0	54.0	47.3	42.3	39.4
200	56.9	51.9	45.2	40.2	37.3
Max Decel (g's)	5.5	11.0	27.6	54.9	81.8

Hgt max q (km)	-gamma (deg)				
beta (kg/m^2)	1	2	5	10	15
25	80.0	75.0	68.3	63.3	60.4
50	75.0	69.9	63.3	58.3	55.4
100	69.9	64.9	58.3	53.2	50.4
150	67.0	62.0	55.3	50.3	47.4
200	64.9	59.9	53.2	48.2	45.3

qmax (W/cm^2)	-gamma (deg)				
beta (kg/m^2)	1	2	5	10	15
25	36.9	52.2	82.5	116.5	142.2
50	52.2	73.9	116.7	164.7	201.1
100	73.9	104.4	165.1	233.0	284.4
150	90.5	127.9	202.2	285.3	348.4
200	104.5	147.7	233.4	329.5	402.3

Qtot (kJ/cm^2)	-gamma (deg)				
beta (kg/m^2)	1	2	5	10	15
25	12.17	8.61	5.45	3.86	3.16
50	17.21	12.17	7.70	5.46	4.47
100	24.34	17.22	10.89	7.72	6.32
150	29.82	21.08	13.34	9.45	7.74
200	34.43	24.35	15.41	10.91	8.94

Table 4.2.2 - Earth deceleration and aeroheating parameters for EDL, for V_∞ = 5 km/s

Hgt Max g (km)	-gamma (deg)				
beta (kg/m^2)	1	2	5	10	15
25	72.0	67.0	60.3	55.3	52.4
50	67.0	62.0	55.3	50.3	47.4
100	61.9	56.9	50.3	45.3	42.4
150	59.0	54.0	47.3	42.3	39.4
200	56.9	51.9	45.2	40.2	37.3
Max Decel (g's)	6.6	13.3	33.2	66.1	98.6

Hgt max q (km)	-gamma (deg)				
beta (kg/m^2)	1	2	5	10	15
25	80.0	75.0	68.3	63.3	60.4
50	75.0	69.9	63.3	58.3	55.4
100	69.9	64.9	58.3	53.2	50.4
150	67.0	62.0	55.3	50.3	47.4
200	64.9	59.9	53.2	48.2	45.3

qmax (W/cm^2)	-gamma (deg)				
beta (kg/m^2)	1	2	5	10	15
25	48.8	69.0	109.1	154.0	188.0
50	69.0	97.6	154.3	217.8	265.8
100	97.6	138.1	218.2	308.0	376.0
150	119.6	169.1	267.2	377.2	460.5
200	138.1	195.2	308.5	435.5	531.7

Qtot (kJ/cm^2)	-gamma (deg)				
beta (kg/m^2)	1	2	5	10	15
25	14.66	10.37	6.56	4.65	3.81
50	20.73	14.66	9.28	6.57	5.38
100	29.32	20.73	13.12	9.30	7.61
150	35.91	25.39	16.07	11.38	9.33
200	41.47	29.32	18.56	13.15	10.77

5. Mars Environment

5.1. Mars Neutral Atmosphere

The following material gives a summary of Mars atmospheric information, including results of some calculations using "back of the envelope" methods presented in Section 2.6. More complete information on atmospheric properties is available in the Mars Global Reference Atmospheric Model (Mars-GRAM) (Justus et al., 2003a; 2004c; Duvall et al., 2005), and in Alexander (2001).

5.1.1. Mars Atmospheric Temperature

Table 5.1.1 shows an abbreviated table of density, temperature, density scale height, and sound speed versus altitude from the Committee on Space Research (COSPAR) Mars Reference

Atmosphere (Pitts et al., 1990). In the calculation of sound speed from equation (2.1.5) or equation (2.1.6), the ratio of specific heats C_p/C_v is 1.33 for Mars.

Table 5.1.1 - Mean density, temperature, density scale height, and sound speed from COSPAR Mars Reference Atmosphere

Height (km)	Temperature (K)	Density (kg/m3)	Density Scale Height (km)	Sound Speed (m/s)
0	214.0	1.550E-02	11.60	233.6
10	205.0	6.470E-03	11.73	228.5
20	188.3	2.630E-03	10.68	218.8
30	175.0	9.800E-04	9.77	211.0
40	162.4	3.400E-04	9.06	203.6
50	152.2	1.080E-04	8.42	197.0
60	144.2	3.180E-05	7.93	191.6
70	139.5	8.730E-06	7.53	188.4
80	139.0	2.290E-06	7.47	187.9
90	139.0	6.010E-07	7.51	188.2
100	139.0	1.590E-07	7.38	188.1
110	149.4	4.140E-08	7.75	195.5
120	159.7	1.190E-08	8.34	202.5
130	170.0	3.760E-09	9.58	208.6
140	245.1	1.090E-09	9.65	251.9
150	288.6	4.730E-10	9.70	275.5

Figure 5.1.1 shows a height-latitude cross section of Mars atmospheric temperature at northern winter solstice (southern summer solstice). This figure illustrates that temperature on Mars varies significantly with height, latitude, and season.

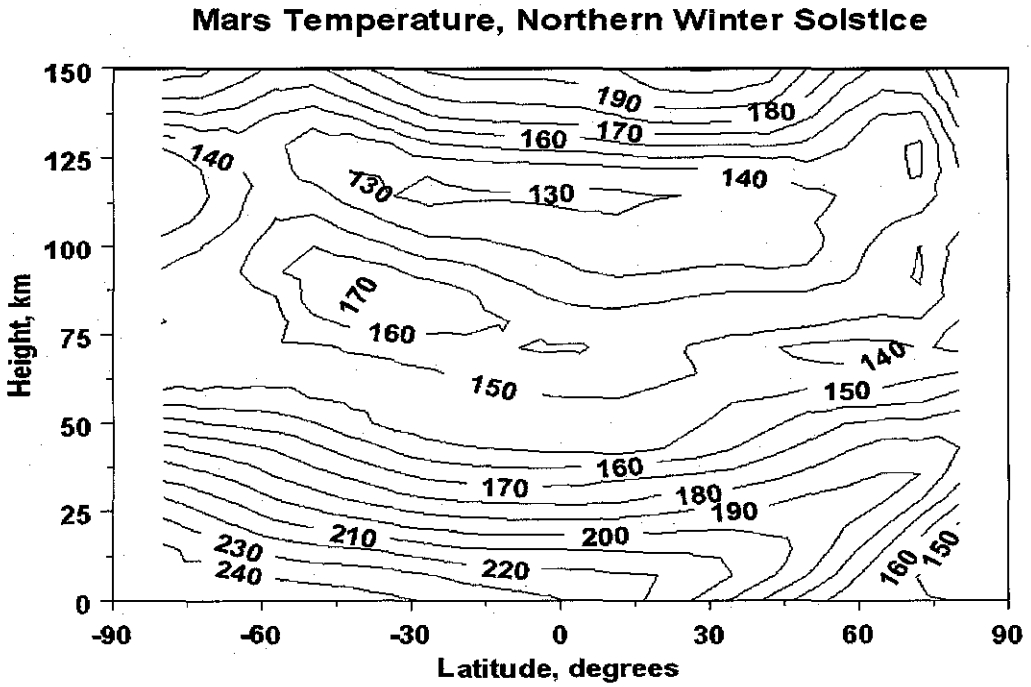

Figure 5.1.1 - Height-latitude cross section of Mars atmospheric temperature at northern winter solstice.

5.1.2. Mars Atmospheric Density

Over the height range 25 km to 70 km, best fit density versus height, assuming constant scale height according to equation (2.3.3), yields $\rho(0) = 3.032E\text{-}2$ kg/m^3 and $H_\rho = 8.757$ km. However, as shown in Figure 5.1.1, this fit does not work well at heights above and below this range.

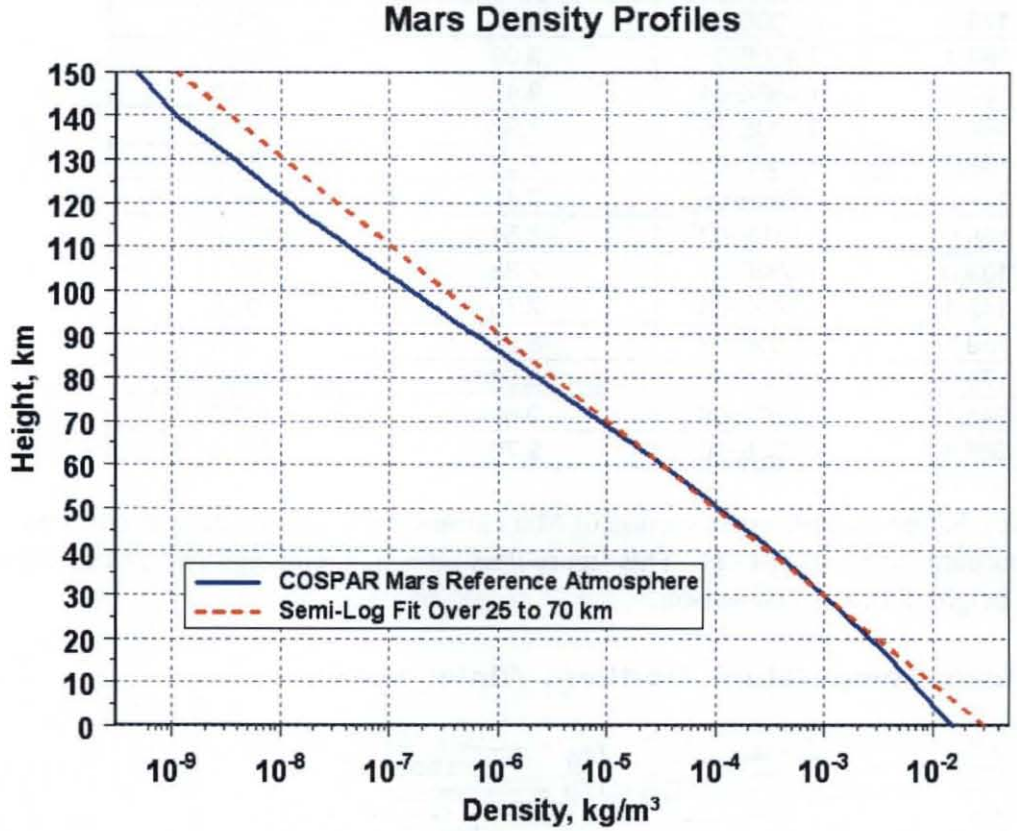

Figure 5.1.2 - COSPAR Mars Reference Atmosphere density profile, compared with best-fit over 25-70 km height range, assuming constant density scale height.

Figure 5.1.3 shows a height-latitude cross section of Mars atmospheric density, expressed as percent deviation from the COSPAR Mars Reference Atmosphere, at northern winter solstice (southern summer solstice). This figure illustrates that density on Mars varies significantly with height, latitude, and season. For this reason, it is suggested that Mars-GRAM (Justus et al., 2003a; 2004c; Duvall et al., 2005) be used to characterize density profiles, rather than relying on a single semi-log profile of the sample density fit used here.

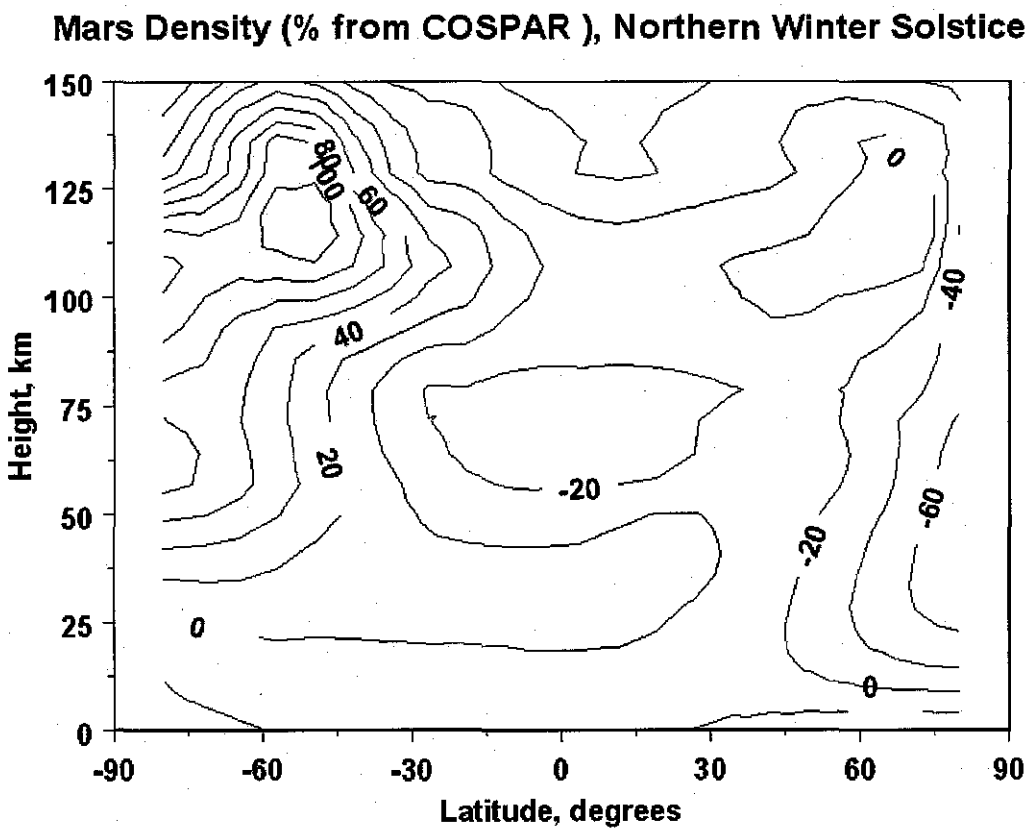

Figure 5.1.3 - Height-latitude cross section of Mars atmospheric density, expressed as percent deviation from the COSPAR Mars Reference Atmosphere.

5.1.3. Mars Density Scale Height

As illustrated by Table 5.1.1 and Figure 5.1.2., density scale height on Mars is not sufficiently constant with altitude for a single semi-log profile of the form given by equation (2.3.3) to apply well at all altitudes. It is recommended that, if using a constant scale height approximation, that the altitude range of the semi-log fit be carefully selected for the specific application involved.

5.1.4. Mars Atmospheric Composition

From the "Mars Fact Sheet" (National Space Science Data Center, 2004), atmospheric composition (mole fraction or volume fraction) near the surface is: carbon dioxide (CO_2) - 95.32% ; nitrogen (N_2) - 2.7%, argon (Ar) - 1.6%; oxygen (O_2) - 0.13%; carbon monoxide (CO) - 0.08%; with minor constituents water vapor (H_2O) - 210 ppm; nitric oxide (NO) - 100 ppm; neon (Ne) - 2.5 ppm; hydrogen-deuterium-oxygen (HDO) - 0.85 ppm; krypton (Kr) - 0.3 ppm; and xenon (Xe) - 0.08 ppm. Near-surface mean molecular mass is 43.34 g/mole (43.34 kg/k-mole).

Above about 100 km altitude, the constituent mix begins to vary with altitude, as given in Figure 5.1.4. Eventually, because of the effects of diffusive separation at very high altitudes, the

atmosphere of Mars becomes primarily atomic hydrogen (H), helium (He), and atomic oxygen (O). At orbital altitudes between about 250 km and 400 km, despite the fact that there is very little free oxygen near the surface of Mars, atomic oxygen is present in large enough concentrations to cause concern for some satellite materials. However, for altitudes of concern for EDL, atomic oxygen is not a factor.

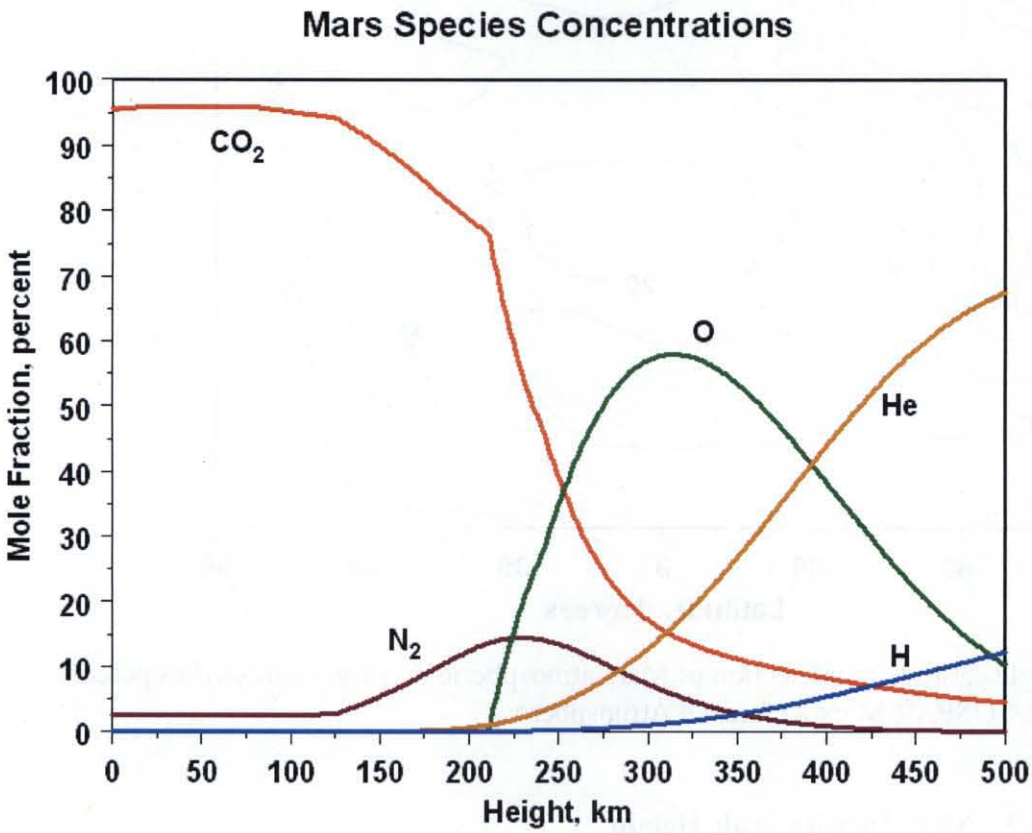

Figure 5.1.4 - Altitude variation of Mars atmospheric constituents.

Dust, in the form of fine-grained particles lofted from the surface of Mars, is an important "constituent" of the atmosphere. Figure 5.1.5 shows a typical (non-dust storm) vertical profile of dust concentration. During large, global-scale dust storms, concentrations could be on the order of ten times the values shown in this figure. Dust is important in affecting the thermal and density structure of the Mars atmosphere, even to much higher altitudes than reached by the actual dust itself. However, dust makes no significant direct contribution to atmospheric density, since dust mixing ratios are typically about 10 parts per million (or 100 parts per million in dust storm cases). Thermal effects (and through these, effects on the atmospheric density profile) can be significant at altitudes well above that reached by the dust itself. See, for example, Figure 3-16 of Alexander (2001).

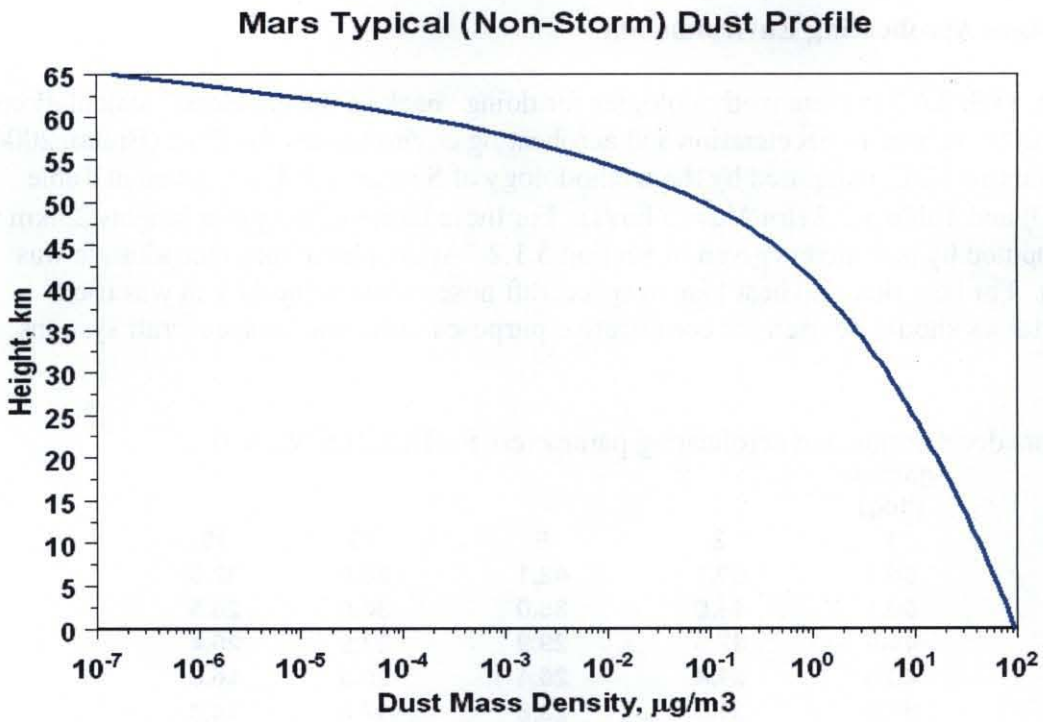

Figure 5.1.5 - Profile of typical (non-dust storm) Mars dust concentration.

5.1.5. Mars Winds

Figure 5.1.6 shows a height-latitude cross section of Mars eastward winds for northern winter solstice (southern summer solstice). This figure shows that Mars winds vary considerably with height, latitude and season. However, comparison with values of sound speed, from Table 5.1.1, shows that winds are a factor only when spacecraft speeds are well below sonic magnitude.

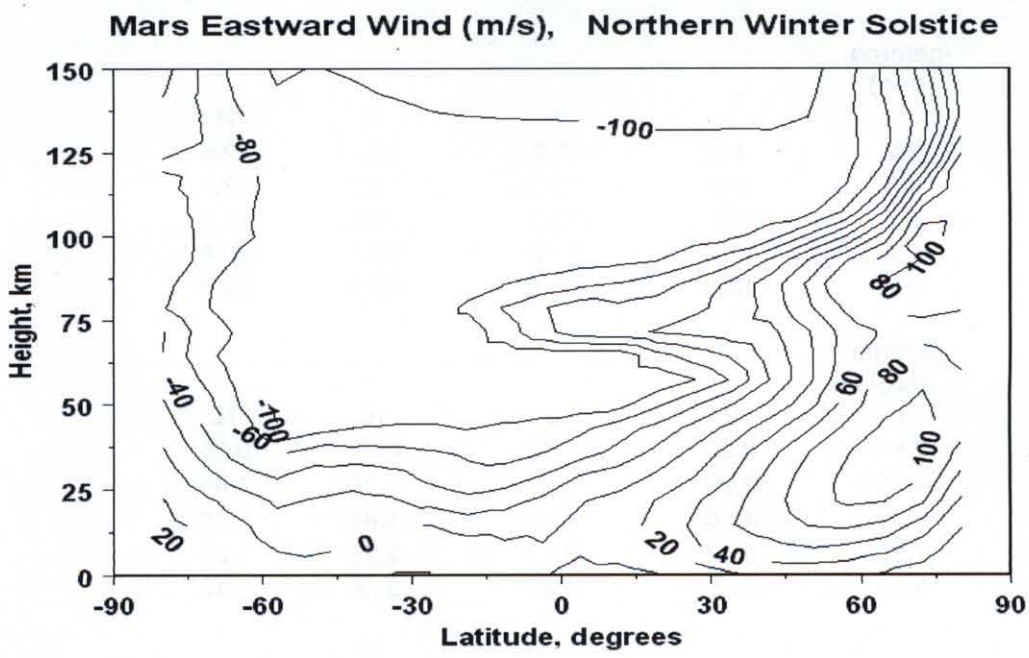

Figure 5.1.6 - Height-latitude cross section of Mars eastward winds for northern winter solstice.

5.2. Mars Aeroheating Environments

Sections 2.6.1 through 2.6.3 present methodologies for doing "back of the envelope" calculations of various parameters related to deceleration and aeroheating environments for EDL (Braun, 2004). Parameters relevant to EDL, computed by the methodology of Section 2.6.1, are given in Table 5.2.1 (for $V_\infty = 0$) and Table 5.2.2 (for $V_\infty = 5$ km/s). For these tables density (for heights 25 km to 70 km) was computed by parameters given in Section 5.1.2. Atmospheric interface altitude was taken as 135 km. For heat flux and heat load, a spacecraft nose radius value of 1 m was used. Results in these tables should be used for comparative purposes only, not for spacecraft systems design.

Table 5.2.1 - Mars deceleration and aeroheating parameters for EDL, for $V_\infty = 0$

Hgt Max g (km)	-gamma (deg)				
beta (kg/m^2)	1	2	5	10	15
25	56.1	50.1	42.1	36.0	32.5
50	50.1	44.0	36.0	30.0	26.5
100	44.0	37.9	29.9	23.9	20.4
150	40.4	34.4	26.4	20.3	16.8
200	37.9	31.9	23.8	17.8	14.3
Max Decel (g's)	0.9	1.8	4.5	9.0	13.4

Hgt max q (km)	-gamma (deg)				
beta (kg/m^2)	1	2	5	10	15
25	65.8	59.7	51.7	45.6	42.1
50	59.7	53.6	45.6	39.6	36.1
100	53.6	47.6	39.5	33.5	30.0
150	50.1	44.0	36.0	30.0	26.5
200	47.5	41.5	33.5	27.4	23.9

qmax (W/cm^2)	-gamma (deg)				
beta (kg/m^2)	1	2	5	10	15
25	3.2	4.6	7.2	10.2	12.5
50	4.6	6.5	10.3	14.5	17.7
100	6.5	9.2	14.5	20.5	25.0
150	7.9	11.2	17.8	25.1	30.6
200	9.2	13.0	20.5	28.9	35.3

Qtot (kJ/cm^2)	-gamma (deg)				
beta (kg/m^2)	1	2	5	10	15
25	2.90	2.05	1.30	0.92	0.75
50	4.10	2.90	1.83	1.30	1.06
100	5.79	4.10	2.59	1.84	1.50
150	7.10	5.02	3.18	2.25	1.84
200	8.19	5.79	3.67	2.60	2.13

These tables give several parameters versus beta [ballistic coefficient β, defined by equation (2.6.3)] and gamma [γ, the flight path angle]. Parameters given are "Hgt Max g" [altitude of maximum g-load, z(gmax) from equation (2.6.10)], "Max Decel" {magnitude of maximum deceleration, gmax from equation (2.6.9)], "Hgt Max q" [altitude of maximum convective heat flux to stagnation point, z(qmax) from equation (2.6.14)], "qmax" [maximum convective heat flux at stagnation point, qmax from equation (2.6.17)], and "Qtot" [total heat load on stagnation point, Q from equation (2.6.19)].

Some heights in these tables, especially for large ballistic coefficient and large magnitude flight path angles, are significantly less than 25 km. Other heights, especially for small ballistic coefficient and small magnitude flight path angles, are close to 70 km. Therefore, density fits over different altitude ranges than 25-70 km might work better in these cases.

Table 5.2.1 - Mars deceleration and aeroheating parameters for EDL, for V_∞ = 5 km/s

Hgt Max g (km)	-gamma (deg)				
beta (kg/m^2)	1	2	5	10	15
25	56.1	50.1	42.1	36.0	32.5
50	50.1	44.0	36.0	30.0	26.5
100	44.0	37.9	29.9	23.9	20.4
150	40.4	34.4	26.4	20.3	16.8
200	37.9	31.9	23.8	17.8	14.3
Max Decel (g's)	1.8	3.7	9.2	18.3	27.3

Hgt max q (km)	-gamma (deg)				
beta (kg/m^2)	1	2	5	10	15
25	65.8	59.7	51.7	45.6	42.1
50	59.7	53.6	45.6	39.6	36.1
100	53.6	47.6	39.5	33.5	30.0
150	50.1	44.0	36.0	30.0	26.5
200	47.5	41.5	33.5	27.4	23.9

qmax (W/cm^2)	-gamma (deg)				
beta (kg/m^2)	1	2	5	10	15
25	9.4	13.3	21.0	29.6	36.1
50	13.3	18.8	29.7	41.9	51.1
100	18.8	26.5	42.0	59.2	72.3
150	23.0	32.5	51.4	72.5	88.5
200	26.5	37.5	59.3	83.7	102.2

Qtot (kJ/cm^2)	-gamma (deg)				
beta (kg/m^2)	1	2	5	10	15
25	5.88	4.16	2.63	1.86	1.53
50	8.32	5.88	3.72	2.64	2.16
100	11.77	8.32	5.26	3.73	3.06
150	14.41	10.19	6.45	4.57	3.74
200	16.64	11.77	7.45	5.27	4.32

6. Titan Environment

6.1. Titan Neutral Atmosphere

The following material gives a summary of Titan atmospheric information, including results of some calculations using "back of the envelope" methods presented in Section 2.6. For more complete information on atmospheric properties, and how they vary with height, latitude, season, etc., the Titan Global Reference Atmospheric Model (Titan-GRAM) is available (Justus et al., 2003b; Duvall et al., 2005).

6.1.1. Titan Atmospheric Temperature

Table 6.1.1 is an abbreviated table of density, temperature, density scale height, and sound speed versus altitude from the Cassini Titan-0 flyby and Titan-A flyby (Titan Atmosphere Model Working Group, personal communication, 2004). For calculation of sound speed, C_p/C_v is 1.40 for Titan.

Table 6.1.1 - Mean density, temperature, density scale height, and sound speed for Titan

Height (km)	Temperature (K)	Density (kg/m3)	Density Scale Height (km)	Sound Speed (m/s)
0	92.89	5.270E+00	27.60	195.6
10	83.29	3.467E+00	22.19	185.7
20	76.44	2.144E+00	19.88	177.7
30	72.20	1.233E+00	17.58	173.1
40	70.51	6.731E-01	16.20	171.5
50	71.16	3.575E-01	15.71	172.5
60	76.62	1.825E-01	13.98	179.2
70	103.46	8.264E-02	13.37	208.4
80	122.88	4.788E-02	20.31	227.1
90	133.97	3.166E-02	25.54	237.1
100	140.80	2.219E-02	28.70	243.1
150	159.23	5.024E-03	36.49	258.6
200	173.76	1.398E-03	40.82	270.1
250	181.72	4.613E-04	48.00	276.2
300	181.72	1.673E-04	50.00	276.2
350	181.72	6.282E-05	51.75	276.2
400	181.72	2.438E-05	53.54	276.2
450	180.81	9.806E-06	56.48	275.5
500	173.96	4.114E-06	57.46	270.2
550	167.06	1.718E-06	57.11	264.8
600	160.09	7.129E-07	56.63	259.3
650	153.04	2.931E-07	55.99	253.5
700	148.62	1.173E-07	53.74	249.8
750	148.62	4.653E-08	54.55	249.8
800	148.62	1.896E-08	56.21	249.8
850	148.62	7.935E-09	57.89	249.8
900	148.62	3.404E-09	59.60	249.8

6.1.2. Titan Atmospheric Density

Over the height range 130 to 800 km, best fit density versus height, assuming constant scale height according to equation (2.3.3), yields $\rho(0) = 1.006E\text{-}1$ kg/m^3 and $H_\rho = 48.38$ km. This height range encompasses all altitudes of interest for maximum g-load and heating for EDL. For final stages, such as parachute deploy and landing, the density profile, given in Table 6.1.1, departs significantly from this semi-log fit, which assumes constant scale height.

6.1.3. Titan Density Scale Height

As shown by Table 6.1.1, density scale height values below about 140 km differ significantly from those at higher altitudes. For this reason, the semi-log fit given above is not applicable below about 130 km.

6.1.4. Titan Atmospheric Composition

Remote sensing data from Cassini Titan-0 and Titan-A flyby operations (Titan Atmosphere Model Working Group, personal communication, 2004) indicate that the Titan atmosphere consists of 97.7% nitrogen (N_2) and 2.3% methane (CH_4). The best available information is that argon concentrations are essentially zero. Near-surface mean molecular mass is 27.32 g/mole (27.32 kg/k-mole). A number of minor species, mostly organic molecules produced from methane-nitrogen photochemistry, are also present in very low concentrations. The N_2/CH_4 ratio of 97.7/2.3 remains essentially constant up until an altitude of about 900 km.

The surface of Titan is shrouded in a permanent haze layer. There is a main haze layer below about 250 km, and a "detached haze layer" at about 350-400 km. Recent Cassini observations have shown much more detailed structure in these haze layers. The haze particles are thought to be of size up to about 1 μm, with concentrations of about 1 g/m^3 to 6 g/m^3, and number densities of up to about 100 cm^{-3}.

6.1.5. Titan Winds

Titan equatorial winds are illustrated in Figure 6.1.1. Winds vary with latitude, but are a maximum at or near the equator. Comparison with values of sound speed, from Table 6.1.1, shows that winds are a factor only when spacecraft speeds are well below sonic magnitude.

6.2. Titan Aeroheating Environments

Sections 2.6.1 through 2.6.3 present methodologies for doing "back of the envelope" calculations of various parameters related to deceleration and aeroheating environments for EDL (Braun, 2004). Parameters relevant to EDL, computed by the methodology of Section 2.6.1, are given in Table 6.2.1 (for $V_\infty = 0$) and Table 6.2.2 (for $V_\infty = 5$ km/s). For these tables, density (for heights 130 km to 800 km) was computed by parameters given in Section 6.1.2. Atmospheric interface altitude was taken as 800 km. For heat flux and heat load, a spacecraft nose radius value of 1 m was used. Results in these tables should be used for comparative purposes only, not for spacecraft design.

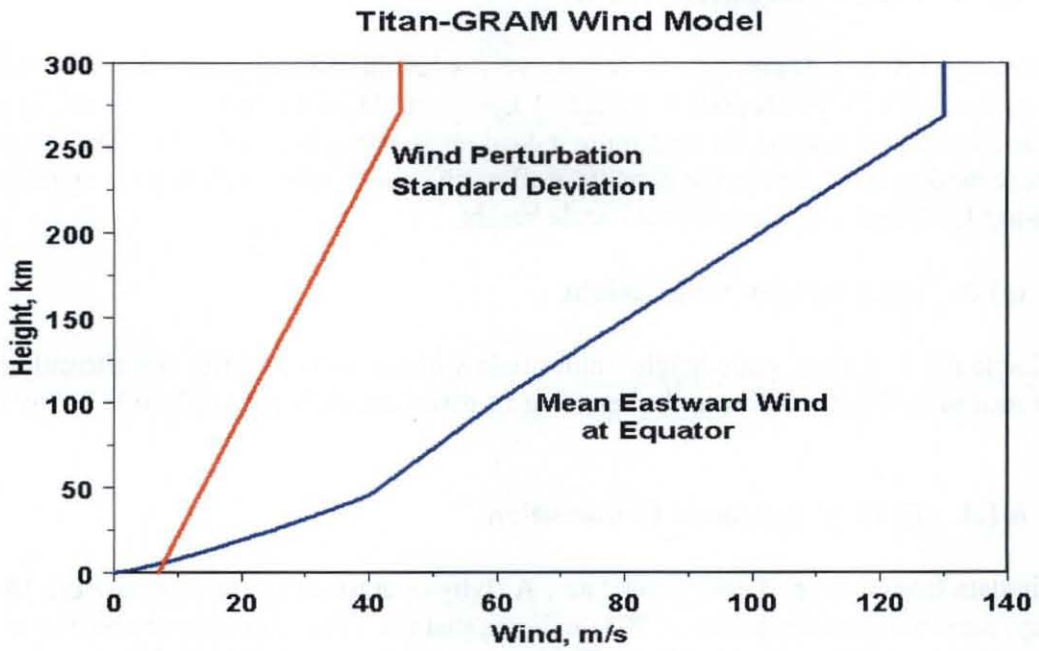

Figure 6.1.1 - Equatorial profile of mean eastward wind and wind standard deviation, from Titan-GRAM (Justus et al., 2003b; Duvall et al., 2005).

These tables give several parameters versus beta [ballistic coefficient β, defined by equation (2.6.3)] and gamma [γ, the flight path angle]. Parameters given are "Hgt Max g" [altitude of maximum g-load, z(gmax) from equation (2.6.10)], "Max Decel" {magnitude of maximum deceleration, gmax from equation (2.6.9)], "Hgt Max q" [altitude of maximum convective heat flux to stagnation point, z(qmax) from equation (2.6.14)], "qmax" [maximum convective heat flux at stagnation point, qmax from equation (2.6.17)], and "Qtot" [total heat load on stagnation point, Q from equation (2.6.19)].

Table 6.2.1 - Titan deceleration and aeroheating parameters for EDL, for $V_\infty = 0$

Hgt Max g (km)	-gamma (deg)				
beta (kg/m^2)	1	2	5	10	15
25	450.9	417.4	373.1	339.7	320.4
50	417.3	383.8	339.5	306.2	286.9
100	383.8	350.3	306.0	272.7	253.3
150	364.2	330.7	286.4	253.0	233.7
200	350.3	316.7	272.5	239.1	219.8
Max Decel (g's)	0.04	0.07	0.18	0.36	0.53

Hgt max q (km)	-gamma (deg)				
beta (kg/m^2)	1	2	5	10	15
25	504.0	470.5	426.2	392.9	373.6
50	470.5	437.0	392.7	359.3	340.0
100	437.0	403.4	359.2	325.8	306.5
150	417.3	383.8	339.5	306.2	286.9
200	403.4	369.9	325.6	292.3	273.0

qmax (W/cm^2)	-gamma (deg)				
beta (kg/m^2)	1	2	5	10	15
25	0.1	0.2	0.3	0.4	0.5
50	0.2	0.2	0.4	0.6	0.7
100	0.2	0.4	0.6	0.8	1.0
150	0.3	0.4	0.7	1.0	1.2
200	0.4	0.5	0.8	1.1	1.3

Qtot (kJ/cm^2)	-gamma (deg)				
beta (kg/m^2)	1	2	5	10	15
25	1.30	0.92	0.58	0.41	0.34
50	1.85	1.30	0.83	0.58	0.48
100	2.61	1.85	1.17	0.83	0.68
150	3.20	2.26	1.43	1.01	0.83
200	3.69	2.61	1.65	1.17	0.96

Table 6.2.2 - Titan deceleration and aeroheating parameters for EDL, for V_∞ = 5 km/s

Hgt Max g (km)	-gamma (deg)				
beta (kg/m^2)	1	2	5	10	15
25	450.9	417.4	373.1	339.7	320.4
50	417.3	383.8	339.5	306.2	286.9
100	383.8	350.3	306.0	272.7	253.3
150	364.2	330.7	286.4	253.0	233.7
200	350.3	316.7	272.5	239.1	219.8
Max Decel (g's)	0.21	0.41	1.02	2.04	3.04

Hgt max q (km)	-gamma (deg)				
beta (kg/m^2)	1	2	5	10	15
25	504.0	470.5	426.2	392.9	373.6
50	470.5	437.0	392.7	359.3	340.0
100	437.0	403.4	359.2	325.8	306.5
150	417.3	383.8	339.5	306.2	286.9
200	403.4	369.9	325.6	292.3	273.0

qmax (W/cm^2)	-gamma (deg)				
beta (kg/m^2)	1	2	5	10	15
25	1.7	2.4	3.8	5.3	6.5
50	2.4	3.4	5.3	7.5	9.2
100	3.4	4.8	7.5	10.6	13.0
150	4.1	5.8	9.2	13.0	15.9
200	4.8	6.7	10.6	15.0	18.4

Qtot (kJ/cm^2)	-gamma (deg)				
beta (kg/m^2)	1	2	5	10	15
25	7.44	5.26	3.33	2.36	1.93
50	10.52	7.44	4.71	3.33	2.73
100	14.87	10.52	6.65	4.71	3.86
150	18.21	12.88	8.15	5.77	4.73
200	21.03	14.87	9.41	6.67	5.46

7. Saturn Environments

7.1. Saturn Neutral Atmosphere

The following material gives a summary of Saturn atmospheric information, including results of some calculations using "back of the envelope" methods presented in Section 2.6. For more complete information on atmospheric properties, and how they vary with altitude, see Lindal et al. (1985), Flasar et al. (2005), and Porco et al. (2005).

7.1.1. Saturn Atmospheric Temperature

Table 7.1.1 is an abbreviated table of density, temperature, density scale height, and sound speed versus altitude for Saturn. In the calculation of sound speed, from equation (2.1.5) or equation (2.1.6), the ratio of specific heats C_p/C_v is taken to be1.45.

Table 7.1.1 – Saturn mean density, temperature, density scale height, and sound speed

Height (km)	Temperature (K)	Density (kg/m3)	Density Scale Height (km)	Sound Speed (m/s)
0	134.8	1.92E-01	69.5	869
20	117.0	1.44E-01	58.0	809
40	100.5	1.02E-01	42.3	749
60	91.1	6.36E-02	36.7	715
80	84.6	3.69E-02	32.4	690
100	82.1	1.99E-02	29.5	678
120	84.1	1.01E-02	28.2	687
140	92.7	4.97E-03	30.1	721
160	104.2	2.56E-03	33.1	764
180	117.6	1.40E-03	38.0	810
200	128.3	8.27E-04	42.9	847
220	136.2	5.19E-04	49.0	873
240	138.6	3.45E-04	48.8	882
260	142.5	2.29E-04	53.9	893
280	141.3	1.58E-04	51.3	890
300	142.6	1.07E-04	53.5	895
350	142.5	4.20E-05	53.5	893
400	142.0	1.65E-05	53.2	892
450	142.0	6.45E-06	53.4	892
500	142.0	2.53E-06	53.3	889
550	142.0	9.91E-07	53.5	891
600	142.0	3.89E-07	53.6	891
650	142.0	1.53E-07	53.7	891
700	142.0	6.03E-08	53.8	891
750	142.0	2.38E-08	53.9	890

7.1.2. Saturn Atmospheric Density

Over the height range 100 to 500 km, best fit density versus height, assuming constant scale height according to equation (2.3.3), yields $\rho(0) =$ 7.45E-2 kg/m^3 and $H_\rho = 47.3$ km. This height range encompasses all altitudes of interest for maximum g-load and heating for EDL. For final stages, such as parachute deploy and landing, the density profile, given in Table 7.1.1, departs significantly from this semi-log fit, which assumes constant scale height.

7.1.3. Saturn Density Scale Height

As shown by Table 7.1.1, density scale height values below about 200 km differ significantly from those at higher altitudes. For this reason, the semi-log fit given above is not applicable below about 100 km.

7.1.4. Saturn Atmospheric Composition

From the "Saturn Fact Sheet" (National Space Science Data Center, 2004), atmospheric composition (mole fraction or volume fraction) near the 1-bar pressure level is: 96.3% molecular hydrogen (H_2) , and 3.25% Helium (He). There are also small amounts (fraction of a percent or less) of methane, ammonia, and other trace species. Mean molecular mass is 2.07 g/mole (2.07 kg/k-mole).

7.1.5. Saturn Winds

Near-equatorial wind speeds of up to 400 m/s occur in the Saturnian atmosphere, while poleward of about 30 degrees latitude, winds are generally less than 150 m/s.

7.2. Saturn Aeroheating Environments

Sections 2.6.1 through 2.6.3 present methodologies for doing "back of the envelope" calculations of various parameters related to deceleration and aeroheating environments for EDL (Braun, 2004). Parameters relevant to EDL, computed by the methodology of Section 2.6.1, are given in Table 7.2.1 (for $V_\infty = 0$). For this tables, density (for heights 100 km to 500 km) was computed by parameters given in Section 7.1.2. Atmospheric interface altitude was taken as 800 km. For heat flux and heat load, a spacecraft nose radius value of 1 m was used. Results in these tables should be used for comparative purposes only, not for spacecraft systems design.

These tables give several parameters versus beta [ballistic coefficient β, defined by equation (2.6.3)] and gamma [γ, the flight path angle]. Parameters given are "Hgt Max g" [altitude of maximum g-load, z(gmax) from equation (2.6.10)], "Max Decel" {magnitude of maximum deceleration, gmax from equation (2.6.9)], "Hgt Max q" [altitude of maximum convective heat flux to stagnation point, z(qmax) from equation (2.6.14)], "qmax" [maximum convective heat flux at stagnation point, qmax from equation (2.6.17)], and "Qtot" [total heat load on stagnation point, Q from equation (2.6.19)].

Table 7.2.1 - Saturn deceleration and aeroheating parameters for EDL, with $V_\infty = 0$

Hgt Max-g (km)	-gamma (deg)				
beta (kg/m^2)	1	2	5	10	15
25	425.6	392.8	349.5	316.9	298.0
50	392.8	360.0	316.7	284.1	265.2
100	360.0	327.2	283.9	251.3	232.4
150	340.8	308.0	264.7	232.1	213.3
200	327.2	294.4	251.1	218.5	199.6
Max Decel (g's)	8.60	17.19	42.94	85.56	127.52

Hgt Max-q (km)	-gamma (deg)				
beta (kg/m^2)	1	2	5	10	15
25	477.5	444.8	401.5	368.9	350.0
50	444.7	412.0	368.7	336.1	317.2
100	412.0	379.2	335.9	303.3	284.4
150	392.8	360.0	316.7	284.1	265.2
200	379.2	346.4	303.1	270.5	251.6

Max-q (W/cm^2)	-gamma (deg)				
beta (kg/m^2)	1	2	5	10	15
25	268.8	380.2	600.8	848.0	1035.3
50	380.2	537.7	849.6	1199.3	1464.2
100	537.7	760.4	1201.6	1696.1	2070.6
150	658.5	931.2	1471.6	2077.2	2536.0
200	760.4	1075.3	1699.3	2398.6	2928.3

Q total (kJ/cm^2)	-gamma (deg)				
beta (kg/m^2)	1	2	5	10	15
25	181.24	128.17	81.10	57.46	47.06
50	256.32	181.26	114.70	81.26	66.56
100	362.49	256.34	162.21	114.92	94.13
150	443.96	313.95	198.66	140.74	115.28
200	512.64	362.52	229.40	162.52	133.12

References

Alexander, M., editor ,"Mars Transportation Environment Definition Document", NASA/TM-2001-210935, 2001.

Allen, H. J., and Eggers, Alfred J., Jr. "A Study of the Motion and Aerodynamic Heating of Ballistic Missiles Entering the Earth's Atmosphere at High Supersonic Speeds", NACA Technical Report 1381, Forty-Fourth Annual Report of the NACA(1958). Washington, D.C.: 1959.

Braun, Robert D., "Planetary Entry, Descent and Landing", Georgia Institute of Technology Short Course, 2004. http://pweb.ae.gatech.edu/people/rbraun/classes/index.html

Duvall, A. L., Justus, C. G., and Keller, V. W., "Global Reference Atmospheric Model (GRAM) Series for Aeroassist Applications", Paper 2005-1239, presented at the 43rd AIAA Aerospace Sciences Meeting, January 10-13, 2005, Reno, Nevada.

Flasar, F. M., et al., "Temperatures, Winds, and Composition in the Saturnian System", *Science Vol. 307.* no. 5713, pp. 1247 – 1251, DOI: 10.1126/science.1105806, 25 February 2005:

Justus, C. G., Duvall, A. L., and Johnson, D. L., "Mars Global Reference Atmospheric Model (Mars-GRAM) and Database for Mission Design", invited paper, presented at the Mars Atmosphere Modeling and Observations Workshop, January 13-15, 2003, Granada, Spain.

Justus, C. G., Duvall, A. L., and Keller, V. W., "Engineering-Level Model Atmospheres for Titan and Mars", invited paper, presented at the International Workshop on Planetary Probe Atmospheric Entry and Descent Trajectory Analysis and Science, October 6-9, 2003, Lisbon, Portugal.

Justus, C. G., Duvall, A. L., and Keller, V. W., "Atmospheric Models for Aerocapture", invited paper, presented at the 40th AIAA/ASME/SAE/ASEE Joint Propulsion Conference, July 12-14, 2004, Ft. Lauderdale, Florida.

Justus, C. G., Duvall, A. L., and Keller, V. W., "Earth GRAM-99 and Trace Constituents", invited paper, presented at the 35th COSPAR Scientific Assembly, July 18-25, 2004, Paris, France.

Justus, C. G., Duvall, A. L., and Keller, V. W., "Validation of Mars-GRAM and Planned New Features", invited paper, presented at the 35th COSPAR Scientific Assembly, July 18-25, 2004, Paris, France.

Kliore, A.J., V. I. Moroz, and G. M. Keating (editors), "The Venus International Reference Atmosphere", *Advances in Space Research, vol. 5*, no. 11, 1985, pages 1-304, Pergamon Press, Oxford, 1986.

Lindal, G. F., D. N. Sweetman, and V. R. Eshleman, "The atmosphere of Saturn: An analysis of the Voyager radio occultation measurements", *Astron. Jour. 90*, 1136–1146, 1985.

National Oceanic and Atmospheric Administration, National Aeronautics and Space Administration, and United States Air Force, "U.S. Standard Atmosphere, 1976", NOAA-S/T 76-1562, 1976.

National Space Science Data Center (NSSDC), "Venus Fact Sheet",
http://nssdc.gsfc.nasa.gov/planetary/factsheet/venusfact.html
"Earth Fact Sheet",
http://nssdc.gsfc.nasa.gov/planetary/factsheet/earthfact.html
"Mars Fact Sheet",
http://nssdc.gsfc.nasa.gov/planetary/factsheet/marsfact.html
"Saturn Fact Sheet",
http://nssdc.gsfc.nasa.gov/planetary/factsheet/saturnfact.html ,
2004.

Pitts, David E., et al., "The Mars Atmosphere: Observations and Model Profiles for Mars Missions", NASA JSC-24455, 1990.

Planetary Data Systems, "Standard Planetary Information, Formulae and Constants", http://atmos.nmsu.edu/jsdap/encyclopediawork.html , 2004.

Porco, C. C., et al., "Cassini Imaging Science: Initial Results on Saturn's Atmosphere", *Science, Vol. 307.* no. 5713, pp. 1243 – 1247, DOI: 10.1126/science.1107691, 25 February 2005

Sutton, K., and Graves, R. A., "A General Stagnation-Point Convective Heating Equation for Arbitrary Gas Mixtures", NASA TR R-376, November 1971.